Twisted accretion curtains in the intermediate polar FO Aquarii

P. A. Evans¹, Coel Hellier¹, Gavin Ramsay² & Mark Cropper² Astrophysics Group, School of Chemistry and Physics, Keele University, Staffordshire, ST5 5BG

- ² Mullard Space Science Laboratory, University College London, Holmbury St. Mary, Dorking, Surrey RH5 6NT

Accepted Received

ABSTRACT

We report on a ~ 37 -ks XMM-Newton observation of the intermediate polar FO Aquarii, presenting X-ray and UV data from the EPIC and OM cameras. We find that the system has changed from its previously reported state of disc-overflow accretion to one of purely disc-fed accretion. We detect the previously reported 'notch' feature in the X-ray spin pulse, and explain it as a partial occultation of the upper accretion pole. Maximum flux of the quasi-sinusoidal UV pulse coincides with the notch, in keeping with this idea. However, an absorption dip owing to the outer accretion curtains occurs 0.27 later than the expected phase, which implies that the accretion curtains are twisted, trailing the magnetic poles. This result is the opposite of that reported in PQ Gem, where accreting field lines were found to lead the pole. We discuss how such twists relate to the accretion torques and thus the observed period changes of the white dwarfs, but find no simple connection.

Key words: Accretion, accretion discs – X-rays: binaries – Stars: individual: FO Agr novae, cataclysmic variables.

INTRODUCTION

FO Agr is an intermediate polar (IP), a magnetic variant of the cataclysmic-variable class of binary stars. These systems consist of a Roche-lobe-filling, late-type secondary and a white-dwarf primary, the latter having a strong magnetic field ($\sim 1-10$ MG), inclined to the rotational axis of the star. The in-falling matter forms an accretion disc which is truncated at the magnetospheric boundary, where it threads onto the white dwarf's magnetic field. The material is then channeled into 'accretion curtains' which guide the material towards the poles, at which stand-off shocks form, heating material to $\sim 10^8$ K (see Patterson 1994 for an in-depth review).

The accretion geometry of FO Aqr has been the subject of much debate (e.g. Hellier 1991; Norton et al. 1992; Hellier 1993; Beardmore et al. 1998; the last three hereafter referred to as N92, H93 and B98 respectively), but it is now generally accepted that the system shows disc-overflow accretion, with most of the material accreting via disc-fed accretion curtains (causing a pulse at the 20.9-min spin cycle), and a component of the accretion stream overflowing the disc and coupling to the magnetic field directly (causing a pulsation at the beat period between the spin and 4.85-hr orbital cycles).

Whereas many IPs have quasi-sinusoidal spin pulses, FO Aqr shows a more complex pulse, including a broader

dip and a narrow 'notch' feature, both of which are variable over time (N92, B98). Our aim here is to use the superior spectroscopic capability of the XMM-Newton satellite to investigate the spin pulse and thus the way in which material leaves the accretion disc and threads onto field lines.

1.1 The spin-cycle ephemeris

The white dwarf in FO Agr was spinning down during the 1980s (Shafter & Macry 1987), but Steiman-Cameron, Imamura & Steiman-Cameron (1989) reported that the periodlengthening had almost stopped by the time of their 1987 observations. Osborne & Mukai (1989) and Patterson et al. (1998) found that FO Aqr then began spinning up, which is confirmed by the most recent ephemeris by Williams (2003). However, these ephemerides suffer from significant O-C jitter and develop a cycle-count ambiguity for times later than 1998 (Williams 2003). Thus we cannot compare the phasing of our data (from 2001) with previous reports with any confidence.

OBSERVATIONS

FO Agr was observed by the XMM-Newton satellite (Jansen et al. 2001) for 37 ks on 2001 May 12. The X-ray MOS-1, MOS-2 (Turner et al. 2001) and PN (Strüder et al. 2001)

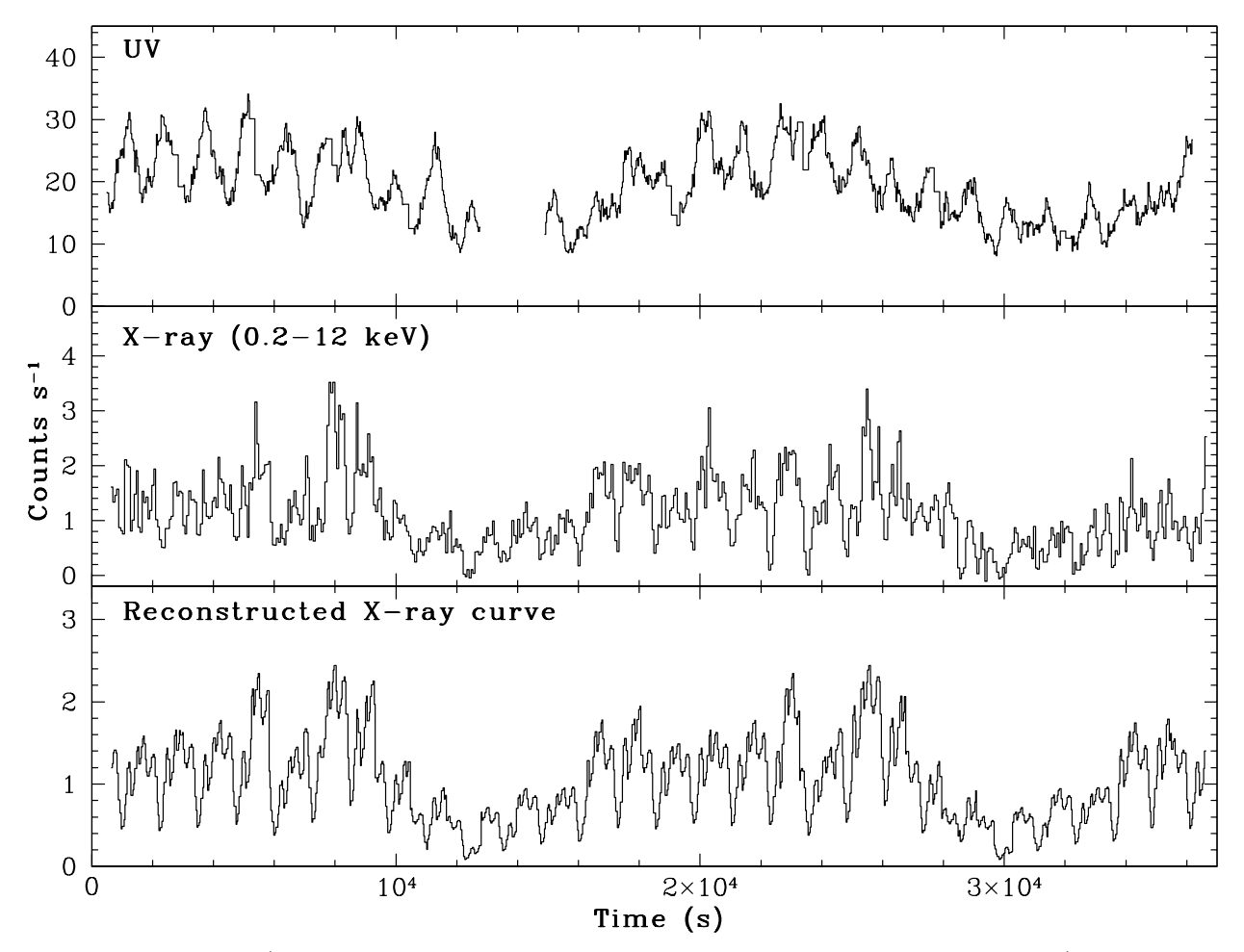


Figure 1. The UV lightcurve (taken with the OM observing through the UVM2 filter and binned at 32 s; top panel) and the EPIC-MOS X-ray lightcurve (binned at 64 s; centre panel). The bottom panel contains the reconstructed model of the X-ray lightcurve, consisting of only spin-cycle and orbital modulations (see text).

cameras were operating in SMALL WINDOW MODE, using the MEDIUM filter. The optical/UV OM camera (Mason et al. 2001) was operating in FAST MODE, observing through the UVM2 filter (2050–2450 Å). The RGS cameras were also in operation; however the count-rate was too low to allow phase-resolved analysis, which is the goal of this paper, thus they are only mentioned in passing here. Some aspects of these data were previously reported by Cropper et al. (2002).

We analysed the data using the XMM-SAS software v5.4.1. The source data were extracted from a circular region of radius 3.5 arcsec enclosing the source, with the background being taken from an annulus around this area. Only single or double pixel events with a zero quality flag were selected.

3 LIGHTCURVES AND POWER SPECTRA

The X-ray and UV lightcurves are presented in Fig. 1, binned at 64 s and 32 s respectively. We show the sum of the MOS lightcurves; the PN lightcurve is very similar to the MOS curves and so is not shown. In any case, the flickering level is higher than the photon noise.

Power spectra of these lightcurves are given in Fig. 2.

The dominant pulses are the 4.85-hr and 20.9-min orbital and spin pulses (we label the frequencies Ω and ω respectively), and there is also power at the $\omega-\Omega$ and $\omega+\Omega$ sidebands.

Power at the beat period $(\omega - \Omega)$ is indicative of spinorbit interaction in the accretion process. X-ray beat periods are generally interpreted as resulting from accreting material which couples directly to the white dwarf magnetosphere, without passing through an accretion disc (e.g. stream-fed accretion, or disc-overflow accretion; Hellier et al. 1989a; Hellier 1991; Wynn & King 1992).

However, we see approximately equal power at the $\omega-\Omega$ and $\omega+\Omega$ sideband frequencies, which may result simply from an amplitude modulation of the spin pulse at the orbital timescale (see Warner 1986), rather than from a stream–magnetosphere interaction. To test this we used the light-curve reconstruction program of H93 to see whether we could reproduce the light curve using a spin pulse multiplied by an orbital modulation, without any intrinsic modulation at the $\omega-\Omega$ period.

The resulting model lightcurve is given in the bottom panel of Fig. 1, and the power spectrum of the residuals to this fitted model is shown in the lower panel Fig. 2. The absence of peaks significantly above the flickering implies that

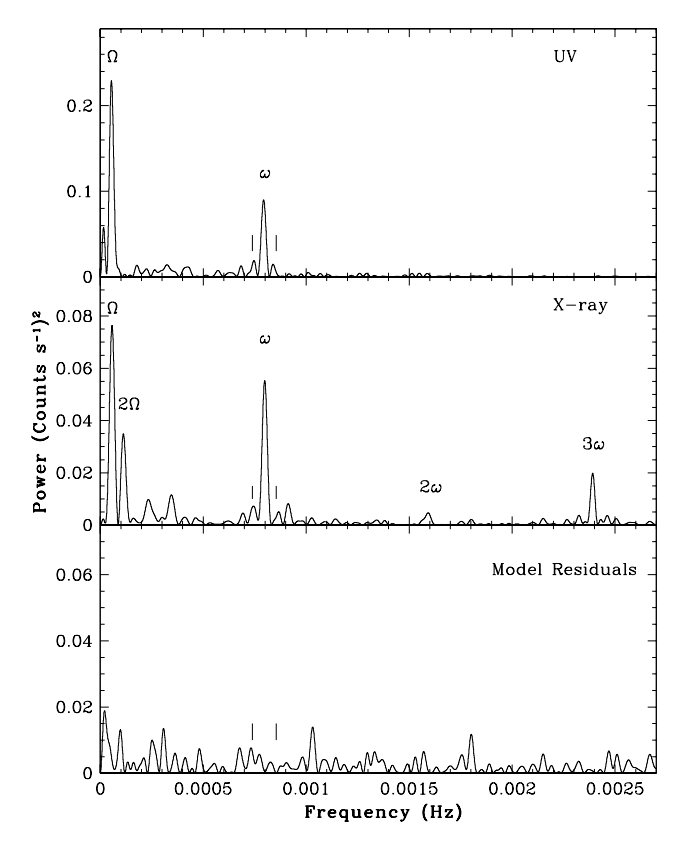


Figure 2. Power spectra of the UV and X-ray (MOS 1+2) data and the model residuals. Ω and ω are the orbital and spin frequencies respectively. The tick-marks indicate the $\omega-\Omega$ and $\omega+\Omega$ sideband frequencies.

the model is adequate in reproducing the periodic components of the lightcurve. Thus we conclude that there was little or no disc-overflow accretion occurring at the time of the *XMM-Newton* observations.

Note that Hellier (1991) and B98 reported that the relative amplitude of the beat and spin pulses change with time, and suggested that the accretion mode of FO Aqr changes from periods with significant disc-overflow accretion to periods where accretion occurs exclusively via the disc. This phenomenon has also been seen in TX Col (Wheatley 1999).

We also note from Fig. 2 that our data show very little power at the 2ω (marked) and 4ω (not shown) frequencies, in contrast to previous data (B98); this indicates substantial changes in the pulse profile over time.

4 SPECTROSCOPY

We extracted phase-averaged source and background spectra from the MOS-1, MOS-2 and PN cameras, and generated response and ancillary response files using the SAS RMFGEN and ARFGEN tasks. We fitted the data from all three cameras simultaneously in XSPEC, making no allowance for calibration systematics between the instruments.

The X-ray emission in an IP arises from plasma which is heated to X-ray temperatures at a stand-off accretion shock, and cools as it approaches the white dwarf surface (e.g. Aizu 1973; Cropper et al. 1999). This can be represented by sev-

eral MEKAL emitters at different temperatures or by using a CEMEKL model, which assumes a continuous power-law distribution of MEKAL emitters.

A single-temperature MEKAL model (plus absorption) gave a fit with $\chi^2_{\nu}=1.64$ and a temperature of 9 keV; adding a second MEKAL improved χ^2 by 18 with temperatures 0.2 keV and 9.3 keV; a third MEKAL improved the χ^2 value by a further 10 ($\chi^2_{\nu}=1.63$), and gave temperatures of 0.2, 3.0 and 14 keV. A fourth MEKAL gave a negligible improvement in χ^2 .

Alternatively, using the CEMEKL model to give a continuous distribution of temperatures resulted in a comparable χ^2_{ν} of 1.64. We use the 3-MEKAL model for phase-resolved analysis below; note, however, that we do not interpret the highest temperature as a shock temperature, since this would require the fitting of a full accretion-column model (e.g. Cropper et al. 1999) and is also affected by the likely presence of a reflection component (e.g. Beardmore, Osborne & Hellier 2000). Instead, the 3-MEKAL model gives an easily-used and flexible representation of the multi-temperature spectrum for studying spectral changes over spin phase.

Blackbody emission may be anticipated in an IP, owing to the heating of the white dwarf surface by the post-shock material, however a blackbody component in the model made negligible difference to the χ^2 value, so was not included.

The spectra show lines of 6.4-keV iron and 0.57-keV oxygen VII that are not reproduced by the 3-MEKAL model (see Fig. 3). The RGS spectrum confirms that the 0.57-keV line is a real feature. In what follows we added narrow Gaussian components to fit these lines.

As is usual in IPs, simple photoelectric absorption was not adequate to fit the spectrum (giving $\chi^2_{\nu}=3.44$ for a simple photoelectric absorber acting on the 3-MEKAL emitter described above). Adding a partial covering absorber gave $\chi^2_{\nu}=1.87$ and a second such component reduced the χ^2_{ν} to 1.63. The fitted parameters of the 3-MEKAL, 3-absorber model are given in Table 1. Note that the amount of absorption changes over spin phase (Section 6) so the parameters fitted to the phase-averaged spectrum will be a weighted average over spin phase.

The above χ^2 values make no allowance for normalisation or calibration systematics between the three instruments. As a test, we have also allowed the parameters of the the 3-MEKAL, 3-absorber model to optimise for each instrument separately. This reduces the overall χ^2_{ν} from 1.63 to 1.03. When we report the phase-resolved analysis we quote $\Delta\chi^2$ values between competing models. Although the absolute χ^2 is lower when allowing the parameters to optimise for each instrument, the $\Delta\chi^2$ values are similar.

One result of the above modelling is the finding of a best-fitting abundance of only 0.12 solar. This results from a relative lack of lines in the data compared to that predicted by the MEKAL code, which assumes that the plasma is optically thin and collisionally ionized. Thus, the different line emission could equally be due to optical depth effects or photo-ionization (see, e.g., Mukai et al. 2003, for such effects in IP spectra). To investigate whether the abundance is genuinely low, or whether the line emission is suppressed, we added a bremsstrahlung emitter for each of the MEKAL emitters with their temperatures fixed to those of the MEKALs; and fixed the abundance to 1 (i.e. solar). This allowed a

4 P. A. Evans et al.

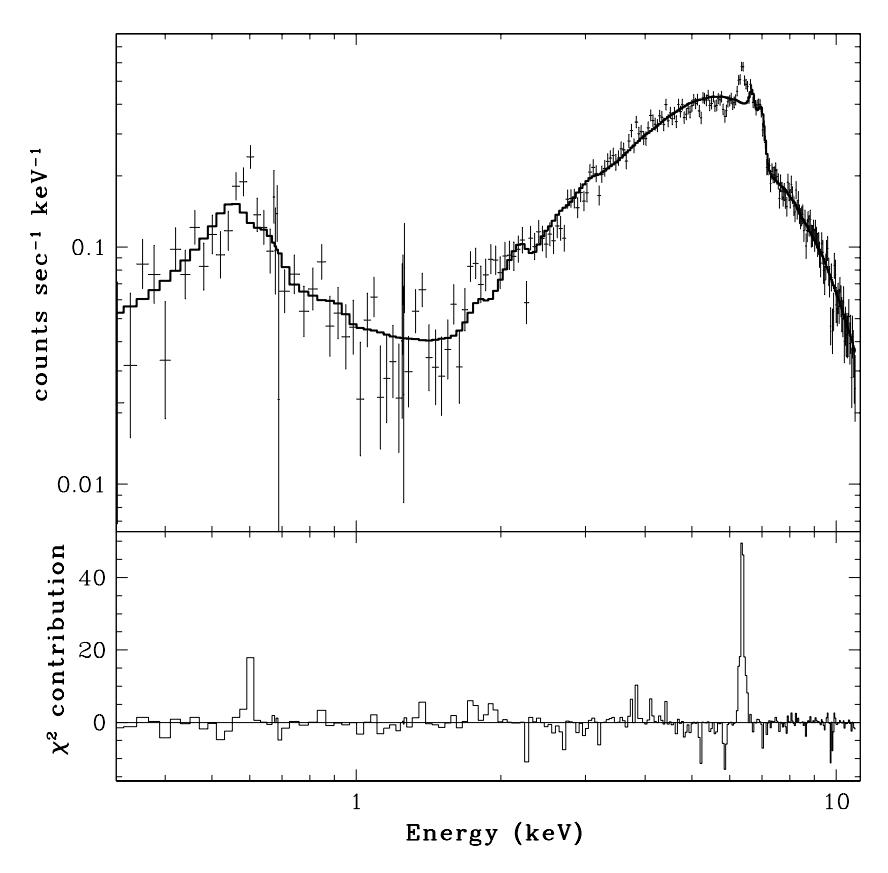


Figure 3. Data, model and residuals of the phase-averaged spectrum from the EPIC-PN camera. The model contains the emitters and absorbers described in the text, but without the Gaussian components. There are two large spikes in the χ^2 panel corresponding to the 6.4-keV iron and 0.57-keV oxygen VII lines, demonstrating the need for these components.

fit to be obtained which was as good as that with a low abundance, but the difference in χ^2 was too low (~ 5) to indicate which of these models is most physical. Applying this model to the higher resolution RGS data showed that either method reproduced the data, provided the abundance was above ~ 0.15 . We use the variable-abundance model in what follows.

5 ORBITAL MODULATION

X-ray observations of FO Aqr often show a prominent modulation on the orbital cycle (e.g. N92), as is obvious in our UV and X-ray data (Fig. 1). The standard interpretation is that FO Aqr is a high-inclination system in which disc material, particularly at the stream–disc impact region, periodically obscures the line of sight to the white dwarf (e.g. H93). Note that Hellier, Mason & Cropper (1989b) reported a grazing optical eclipse in FO Aqr, implying an inclination of $\sim 65^{\circ}$, although there is no sign of the white dwarf itself being eclipsed.

Other possible causes of an orbital modulation include stream-fed accretion in which the accretion footprints are linked to orbital phase (N92). This, though, is less able to explain our dataset given the absence of the X-ray beat modulation that would also result (Section 3).

Fig. 4 shows a softness-ratio plot of the orbital modulation, constructed using 1254-s bins to smooth out the spin

pulse (we show the data unfolded since we have only ~ 2.1 orbital cycles of data). The softness ratio closely follows the lightcurve, implying that the spectrum gets harder in the minima, supporting the absorption idea.

To investigate further we extracted spectra from the three X-ray cameras in the orbital dip ($\phi=0.85$ –1.2) and out of the dip ($\phi=1.2$ –0.85). Fitting the spectra with the model discussed in Section 4, we found that the spectra were adequately reproduced by a model in which only the absorption changed during the dip. This required increased partial-covering absorbers with a density near 3×10^{23} cm⁻², and gave a best-fitting χ^2_{ν} of 1.37 (with much of the excess χ^2 arising from systematics between the three X-ray cameras). Allowing other parameters to vary in addition to the absorption improved the χ^2 by only 18 (for $\nu=2164$), which is not significant.

From the softness ratio and spectral modelling, and the absence of beat-cycle modulations, we conclude that the orbital modulation is a 'dipping' event resulting from absorption by stream or disc material. The material must extend to $\gtrsim 25^{\circ}$ above the plane, given the inclination quoted above, and must extend for at least 0.4 in orbital phase. This suggests that the stream/disc interaction region is quite extensive.

Component	Parameter (Units)	Value	Error
Absorption	nH (cm ⁻²)	1.02×10^{21}	$+0.81 \times 10^{21}$ -0.05×10^{21} $+0.12 \times 10^{23}$
Partial Absn.	nH (cm ⁻²) CvrFract	1.90×10^{23} 0.855	$-0.09 \times 10^{23} +0.021 \\ -0.026 \times 10^{-2}$
Partial Absn.	nH (cm ⁻²) CyrFract	5.71×10^{22} 0.980	$+0.45 \times 10^{22}$ -0.41×10^{22} $+0.004$
Gaussian	Energy (keV)	6.40	-0.005 FROZEN $+0.695 \times 10^{-5}$
	Normalisation Eq. width (eV)	9.23×10^{-5} 129	-1.41×10^{-5}
Gaussian	Energy (keV) Normalisation	0.587 6.84×10^{-3}	$^{+0.031}_{-0.029}$ $^{+4.69 \times 10^{-3}}$
	Eq. width (eV)	22.9	-4.54×10^{-3} +0.024
Mekal	kT (keV) Abundance	$0.176 \\ 0.121$	-0.024 -0.026 $+0.028$ -0.023
Mekal	Normalisation kT (keV)	0.160 3.00	+0.365 -0.094 $+1.48$
	Normalisation	3.32×10^{-2}	-0.73 $+1.87 \times 10^{-2}$ -1.51×10^{-2}
Mekal	kT (keV) Normalisation	$13.9 \\ 4.02 \times 10^{-2}$	$+6.5$ -3.1 $+0.88 \times 10^{-2}$ -1.06×10^{-2}

Table 1. Model components and parameters fitted to the phase-averaged spectrum. The errors show the 90% confidence limit, according to formal statistics, making no allowance for calibration uncertainties between the three detectors.

6 SPIN MODULATION

Fig. 5 shows the UV and summed X-ray lightcurves folded on the 1254-s spin period, along with the softness ratio of the X-ray data. We have phased our data such that spin-phase zero occurs at the maximum of the UV pulse, located by fitting a sine curve to those data. This phase zero corresponds to 0.23 on the Williams (2003) ephemeris.

The X-ray pulse profile shows a main dip (at phase 0.75 on our plots) followed by a 'notch' feature (phases 0.0–0.1), which concurs with previous reports by N92, H93, and B98. The softness ratio of the X-ray spin pulse follows the morphology of the total flux level.

6.1 Spectral analysis

To investigate the spin-pulse features noted above we extracted spectra from all three X-ray cameras from spin 'maximum' ($\phi \sim 0.12$ –0.36), 'minimum' ($\phi \sim 0.67$ –0.87), and the 'notch' ($\phi \sim 0.99$ –1.11). We applied the three-MEKAL model described in Section 4 simultaneously to 'maximum' and 'minimum', allowing the parameters to vary between regions, and then fixing the emission or absorption, in order to investigate the probable cause of the changes. We then repeated this process between the 'maximum' and 'notch' phase regions. XSPEC could not always constrain the MEKAL temperatures, so we froze these at 0.1, 2 and 30 keV as this had negligible effect on the fit quality. We also tied the abundance across phase regions, since it had a minimal effect on the fit quality ($\Delta \chi^2 \sim 5$), and fixed the 0.57-keV line at its rest energy with zero width.

Fitting the maximum and minimum phase regions simultaneously without requiring any model parameters to

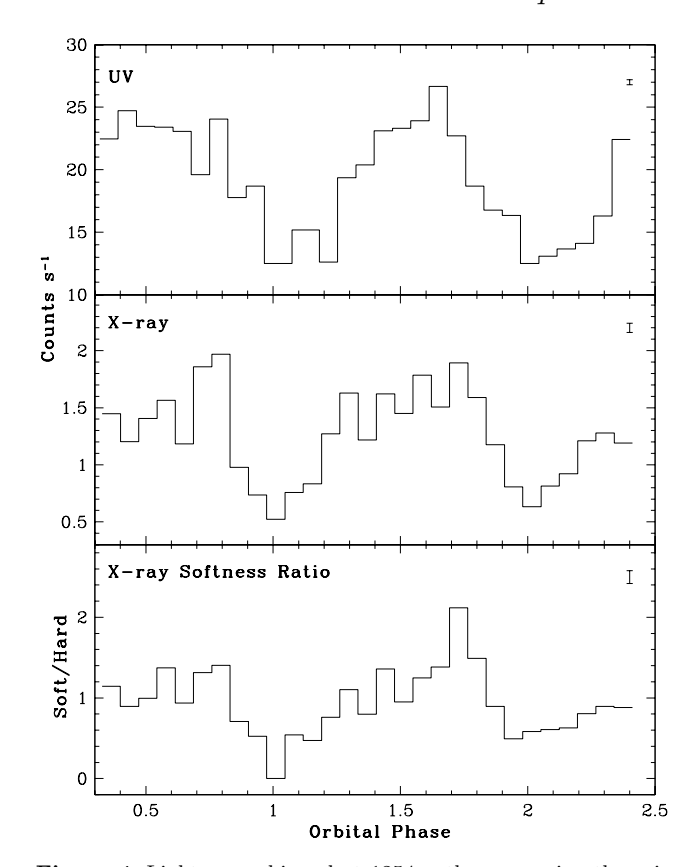


Figure 4. Lightcurves binned at 1254 s, thus removing the spin modulation. The data are not folded but are plotted against phase. The top two panels show the UV (OM) and the X-ray (MOS 1+2) data. The bottom panel shows the MOS 1+2 softness ratio, defined as 0.2-4/6-12 keV. Typical error bars are shown. Phase zero occurs at HJD 2452041.806, and has been defined as the minimum of the UV pulse, estimated by eye.

be the same (with the exceptions noted above) yielded a best-fitting model of $\chi^2_{\nu}=1.2~(\nu=1161)$. Note, again, that much of the χ^2 comes from calibration uncertainties; optimising for each instrument separately gave $\chi^2_{\nu}=0.87$. Since these systematics dominate χ^2 , true uncertainties are much greater than the probabilities drawn from formal statistics; thus we present our results using $\Delta\chi^2$ values rather than probabilities.

Constraining the model so that the absorption could not vary between maximum and minimum made the fit worse by $\Delta \chi^2 = 53$; if instead the absorption is allowed to vary and the emission parameters are fixed, the fit is worse by $\Delta \chi^2 = 29$. This suggests that the minimum is mostly the result of absorption.

We then fitted the maximum and notch simultaneously: allowing only the absorption to vary worsened the fit by $\Delta\chi^2=39$ compared to an unconstrained model, whereas allowing only the emission parameters to vary worsened the fit by only $\Delta\chi^2=4$. From this we conclude that the notch is probably not an absorption event, but is caused by a change in the underlying emission, such as the occultation of parts of the accretion region.

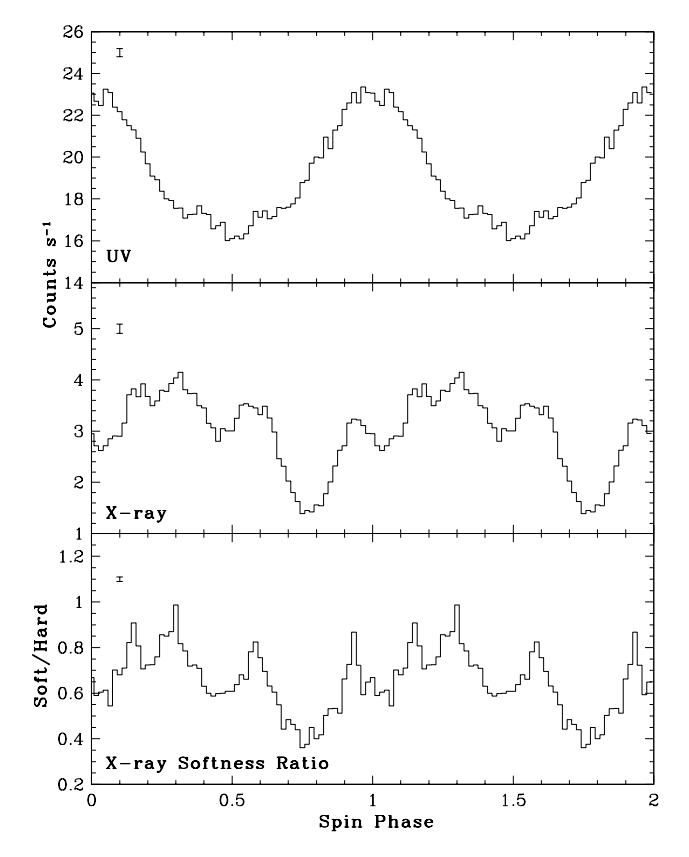


Figure 5. Spin pulse profiles, folded on ω =1254.4459 s. Phase zero occurs at HJD 2452041.858. The upper panel shows the UV (OM) data. The central panel shows the X-ray (MOS+PN) data, and the 0.2–4 / 6–12 keV softness ratio is in the lower panel. Typical errors are given.

7 DISCUSSION

FO Aqr has a complex X-ray spin-pulse profile. The main feature is a dip, centered at $\phi \sim 0.75$, which is caused by increased absorption (section 6.1). Strong absorption dips are characteristic of IPs, and in the standard model occur when the accretion curtains of infalling material obscure the line of sight to the accretion regions (e.g. Rosen, Mason & Córdova 1988; Hellier, Cropper & Mason 1991; Kim & Beuermann 1995).

Our data also show a smaller flux reduction, the 'notch' at $\phi \sim 0.0$. This notch is persistent in FO Aqr's X-ray lightcurve (e.g. N92, B98) and is often more prominent than in our data. Our spectral analysis suggests that this is the disappearance of part of the emitting region, rather than an absorption dip.

N92 attributed the notch to the disappearance over the white-dwarf limb of a 'hot-spot' within the accretion region at the upper pole. H93 suggested that it is probably the upper pole itself that disappears: the width of the notch implies a region covering 0.001 of the white-dwarf area (N92), which is in line with the estimate of < 0.002 for the size of the accreting poles in the eclipsing system XY Ari (Hellier 1997a).

Our simultaneous far-UV light curve shows a nearly-sinusoidal spin pulse with a maximum coincident with the notch $(\phi \sim 0.0).$ In the standard accretion-curtain model, the optical and UV maximum occurs when the upper pole is on the far side of the white dwarf, furthest from the observer, and the accretion curtains are best displayed (Hellier et al. 1987). This is consistent with our interpretation of the notch. We do, though, require an asymmetry in the visibility of the upper and lower poles, otherwise the appearance of the lower pole would compensate for the disappearance of the upper pole and fill in the notch. This point was previously noted by B98, who showed that the notch lightcurve could be reproduced if the magnetic dipole were offset by 0.15 white-dwarf radii from the centre.

Given the above, a simple model would predict that the absorption dip caused by the upper accretion curtain passing through the line of sight would occur half a cycle later, at $\phi \sim 0.5$. In fact, it occurs at $\phi \sim 0.77$, late by 0.27 cycles. A simple shift in phase, such as accreting only along field lines trailing the pole, would not by itself explain the quarter-cycle discrepancy between phases deduced from the UV and the X-ray. Thus we conclude that the field lines are not an undistorted dipole, but are twisted, being swept backwards by a quarter of a cycle.

We can use B98's compilation of FO Aqr lightcurves to investigate whether the amount of distortion is variable over time. The notch is prominent in Ginga data taken in 1988 and 1990, and in both cases implies an accretion-curtain lag comparable to the amount we see in our data. The notch is either less obvious or absent in EXOSAT data from 1983 and 1985, and in ASCA data from 1993, but the statistical quality of those lightcurves is much lower. Thus, where both a notch and a dip are seen, the phase-difference between them is compatible with a constant lag, and there is no evidence for episodes when the accretion-curtain twist is markedly different.

7.1 Comparison with PQ Gem

While many intermediate polars have quasi-sinusoidal spin pulses, PQ Gem, like FO Aqr, has a more complex pulse (e.g. Mason 1997). However, in that star it is proposed that the accreting field lines *precede* the magnetic pole, the opposite to our conclusion for FO Aqr, based on analysis of the X-ray pulse (Mason 1997), optical polarimetry (Potter et al. 1997), and optical spectroscopy (Hellier 1997b).

A possible line of enquiry is whether the twists in the accretion curtains – opposite in the two stars – are related to the accretion torques on the white dwarfs. In PQ Gem the white dwarf is spinning down on a 2.4×10^4 -yr timescale (Mason 1997). FO Aqr's white dwarf has shown a more complex history, having been spinning down between 1981 and 1988, after which it changed to spinning up (Williams 2003).

The spin-pulse profiles of FO Aqr have varied over that time period (e.g. B98), however there is no simple change in the relative locations of dip and notch that could be attributed straightforwardly to the change from spin down to spin up. Thus, although it is tempting to note that in the spinning-down PQ Gem the field lines precede the magnetic pole, whereas in the (currently) spinning-up FO Aqr they trail the magnetic pole, any deductions from this are not straightforward.

Ghosh & Lamb (1979) argue that the net accretion torque on the white dwarf combines the spin-up torque from the angular momentum of the accreted material with the torques of field lines dragging through the accretion disc. The expected result is a spin period which oscillates around an equilibrium period, undergoing phases of spin up and spin down. The field–disc torques could be the cause of the twists in the accretion curtains.

Mason (1997) and Potter et al. (1997), on the basis of optical polarimetry, proposed that in PQ Gem the accreting material threads field lines outside the corotation radius (where the field lines are moving faster than the disc material) and that this leads to the spin-down seen in that star. However, Mason (1997) notes that accretion from outside the corotation radius contradicts the standard theory of how an accretion disc interacts with a magnetic field (e.g. Ghosh & Lamb 1979). Our results from FO Aqr mean that the theory must also be adaptable to explain accretion along trailing field lines, and also the puzzling fact that the lines appear to trail both in episodes of spin-up and of spin-down. Thus any interpretations of the field twists seen in PQ Gem and FO Aqr are currently uncertain.

8 CONCLUSIONS

Analysis of XMM-Newton data on FO Aqr has shown that at the time of our observations:

- (1) There was negligible disc-overflow accretion.
- (2) An orbital dip was probably caused by absorption of the X-ray emission by vertical structure in the accretion disc.
- (3) A narrow 'notch' in the X-ray spin pulse is likely to be caused by the upper accretion region disappearing over the limb of the white dwarf.
- (4) The UV spin pulse is quasi-sinusoidal with a maximum coincident with the notch. This will occur when the base of the upper pole is furthest from us, and accords with the accretion curtain model for UV/optical spin pulses.
- (5) A broad dip in the X-ray pulse is caused by absorption, most likely occurring when the outer regions of the upper accretion curtain cross our line of sight to the white dwarf.
- (6) The phase difference between the broad dip and the notch is 0.23, whereas a simple accretion-curtain model would predict 0.5. This implies that the curtains are twisted, with the outer parts trailing the magnetic pole.
- (7) The finding of a trailing curtain contrasts with reports that the accretion curtains lead the magnetic poles in PQ Gem.
- (8) Although PQ Gem's white dwarf is spinning down, whereas that in FO Aqr is (currently) spinning up, there appears to be no simple relation between the period change and whether the curtain trails or leads.

REFERENCES

Aizu K., 1973, Prog. Theor. Phys., 49, 1184

Beardmore A.P., Mukai K., Norton A.J., Osborne J.P., Taylor P., 1996, MPE Report, 263, 123

Beardmore A.P., Mukai K., Norton A.J., Osborne J.P., Hellier C., 1998, MNRAS, 297, 337 (B98)

Beardmore A.P., Osborne J.P., Hellier C., 2000, MNRAS, 315, 307

Cropper M., Wu K., Ramsay G., Kocabiyik A., 1999, MNRAS, 308, 807 Cropper M., Ramsay G., Hellier C., Mukai K., Mauche C., Pandel D., 2002, Phil Trans R Soc Lond A, 360, 1951

Ghosh P., Lamb F.K., 1979, ApJ, 234, 296

Hellier C., 1991, MNRAS, 251, 693

Hellier C., 1993, MNRAS, 265, L35 (H93)

Hellier C., 1997a, MNRAS, 291, 71

Hellier C., 1997b, MNRAS, 288, 817

Hellier C., Mason K.O., Rosen S.R., Córdova F.A., 1987, MN-RAS, 228, 463

Hellier C., Mason K.O., Smale A.P., Corbet R.H.D., O'Donoghue D., Barrett P.E., Warner B., 1989a, MNRAS, 238, 1107

Hellier C., Mason K.O., Cropper M., 1989b, MNRAS, 237, 39

Hellier C., Cropper M., Mason K.O., 1991, 248, 233

Jansen F. et al., 2001, A&A, L1

Kim Y., Beuermann K., 1995, A&A, 298, 165

Mason K.O., 1997, MNRAS, 285, 493

Mason K.O. et al., 2001, A&A, 365, L36

Mukai K., Kinkhabwala A., Peterson J.R., Kahn S.M., Paerels F., 2003, ApJ, 586, L77

Norton A.J., Watson M.G., King A.R., Lehto H.J., McHardy I.M., 1992, MNRAS, 254, 705 (N92)

Osborne J.P., Mukai K., 1989, MNRAS, 238, 1233

Patterson J., 1994, PASP, 106, 209

Patterson J. et al., 1998, PASP, 110, 415

Potter S.B., Cropper M., Mason K.O., Hough J.H., Bailey J.A., 1997, MNRAS, 285, 82

Rosen S.R., Mason K.O., Córdova F.A., 1988, MNRAS, 231, 549 Shafter A.W., Macry J.D., 1987, MNRAS, 228, 193

Steiman-Cameron T.Y., Imamura J.N., Steiman-Cameron D.V., 1989, ApJ, 339, 434

Strüder L. et al., 2001, A&A, 365, L18

Turner M.J.L. et al., 2001, A&A, 365, L27

Warner B., 1986, MNRAS, 219, 347

Wheatley P.J., 1999, in Hellier C., Mukai K., eds, ASP Conf. Ser. Vol 157, Annapolis Workshop on Magnetic Cataclysmic Variables. Astron. Soc. Pac., San Francisco, p. 47

Williams G., 2003, PASP, 115, 618

Wynn G.A., King A.R., 1992, MNRAS, 255, 83